THE FASEB JOURNAL • RESEARCH • www.fasebj.org

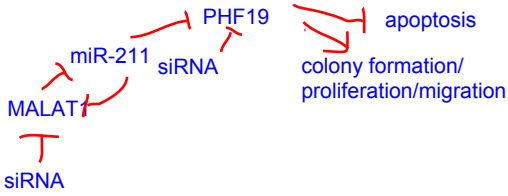

miR-211 sponges lncRNA MALAT1 to suppress tumor growth and progression through inhibiting PHF19 in ovarian carcinoma

Fangfang Tao,[*,1] Xinxin Tian,[†,‡,1] Shanming Ruan,[§] Minhe Shen,[§] and Zhiqian Zhang[‡,¶,2]

[*]Department of Immunology and Microbiology, Basic Medical College, Zhejiang Chinese Medical University, Hangzhou, China; [†]Department of Biochemistry and Biophysics, Texas A&M AgriLife Research, Texas A&M University, College Station, Texas, USA; [‡]Tianjin International Joint Academy of Biomedicine (TJAB), Tianjin, China; [§]Department of Medical Oncology, First Affiliated Hospital of Zhejiang Chinese Medical University, Hangzhou, China; and [¶]State Key Laboratory of Medicinal Chemical Biology, Nankai University, Tianjin, China

ABSTRACT: Accumulating evidence has indicated that microRNAs (miRNAs) play an important role in the occurrence and progression of ovarian cancer (OC). However, the function of miRNAs implicated in OC remains unclear. This study investigated the potential role of miR-211 in OC. Gene Expression Omnibus database analysis indicated that miR-211 expression was significantly down-regulated in OC tissues compared with normal specimens. In addition, miR-211 overexpression apparently inhibited proliferation, migration, xenograft growth, and induced apoptosis in HEY-T30 and SKOV3 cells. Moreover, PHF19, a component of the polycomb group of proteins, was found to be a direct target of miR-211 based on the luciferase reporter assay and Western blot analysis. Consistently, survival analysis indicated that high PHF19 expression was associated with shorter survival time in patients with OC. Importantly, silence of PHF19 reduced proliferation, induced cell cycle arrest, promoted apoptosis, suppressed migration, and inhibited xenograft growth in SKOV3 cells. Restoration of PHF19 expression markedly reversed the inhibitory effect of miR-211 on OC. Moreover, our results indicate that the long noncoding RNA MALAT1 could sponge miR-211 as a competing endogenous RNA and potentially up-regulate PHF19 expression, thus facilitating the OC progression. These findings suggest that the MALAT1/miR-211/PHF19 axis may act as a key mediator in OC and provide new insight into the prevention of this disease.—Tao, F., Tian, X., Ruan, S., Shen, M., Zhang, Z. miR-211 sponges lncRNA MALAT1 to suppress tumor growth and progression through inhibiting PHF19 in ovarian carcinoma. FASEB J. 32, 6330–6343 (2018). www.fasebj.org

KEY WORDS: ovarian cancer · MiR-211 · PHF19 · MALAT1 · ceRNA

Ovarian cancer (OC) is the second leading cause of cancer-associated deaths worldwide among gynecologic malignancies. Due to a lack of effective early screening methods, patients with OC are frequently diagnosed at the advanced stage of disease. In addition, tumor recurrence frequently occurs in the majority of patients with OC who undergo surgery followed by chemotherapy at a median of 15 mo from diagnosis (1). Most deaths from this disease are attributed to remote metastasis, and the 5-yr survival rate for patients with OC remains <30% (2–4). Conversely, the mechanisms underlying OC cell proliferation, migration, and metastasis have not been fully defined. Therefore, understanding the molecular events and exploring the precise processes of OC initiation, progression, and metastasis are critical to developing new strategies for the treatment of OC.

As a class of small endogenous nonprotein-coding RNAs, microRNAs (miRNAs) suppress cellular protein expression by binding the 3′-untranslated regions (3′-UTRs) of target mRNAs (5, 6). Accumulating evidence has shown that miRNAs play key roles in multiple physiologic and pathologic processes, including cancer initiation, progression, and metastasis. A wide range of miRNAs have been reported to be up-regulated or down-regulated in OC and involved in the pathogenesis of OC (6–8). For instance, miR-34a reportedly suppresses OC cell proliferation and chemoresistance *via* targeting HDAC1 (9). MiR-409-3p decreases cisplatin sensitivity of OC cells through blocking cellular autophagy mediated by Fip200 (10). MiR-211, an miRNA encoded by the sixth intron of the TRPM1 gene at 15q13-q14, has been observed to be deregulated in many

ABBREVIATIONS: ceRNA, competing endogenous RNA; GAPDH, glyceraldehyde-3-phosphate dehydrogenase; GEO, Gene Expression Omnibus; lncRNA, long noncoding RNA; MALAT1, metastasis-associated lung adenocarcinoma transcript 1; miRNA, microRNA; mut, mutant; OC, ovarian cancer; shRNA, short hairpin RNA; TCGA, The Cancer Genome Atlas; 3′-UTR, 3′-untranslated region; WT, wild type

[1] These authors contributed equally to this work.

[2] Correspondence: Tianjin International Joint Academy of Biomedicine (TJAB), Tianjin 300457, China. E-mail: zhangzhiqian@tjab.org

doi: 10.1096/fj.201800495RR

This article includes supplemental data. Please visit *http://www.fasebj.org* to obtain this information.

0892-6638/18/0032-6330 © FASEB

tumors (11–15). For instance, miR-211 has strong inhibitory effects on melanoma cell growth, invasion, and metastasis. However, only 1 publication has mentioned the role of miR-211 in OC until now. In that paper, Xia *et al.* (16) found that miR-211 inhibits OC proliferation and induces cell cycle arrest by suppressing CCND1 and CDK6, but its function and underlying mechanisms in OC invasion, migration, and metastasis remain unknown.

Long noncoding RNAs (lncRNAs) represent a class of nonprotein-coding RNAs whose transcripts are >200 nt in length (17). Recent studies have shown that lncRNAs contribute to the pathogenesis of multiple human diseases and tumorigenesis of various cancers (17, 18). In OC, some lncRNAs are up-regulated as oncogenes, such as MALAT1 and TUG1, whereas others are down-regulated and act as tumor suppressors, including BC200 and GAS5 (19–23). Mechanistically, lncRNAs can interact with miRNAs to form competing endogenous RNAs (ceRNAs) and regulate each other's expression with the miRNA response elements (24–26). An increasing body of studies has shown that the function of most lncRNAs in carcinogenesis is mediated by ceRNA crosstalk (26–28). For instance, NEAT1 sponges miR-194 to regulate paclitaxel resistance of OC cells through up-regulating ZEB1 expression (29). Metastasis-associated lung adenocarcinoma transcript 1 (MALAT1) is one of the highly conserved lncRNAs that has extensive functions in the formation and progression of most types of cancers (30–33). In OC, Pa *et al.* (19) indicated that MALAT1 promotes viability, invasion, and migration of OC cells by regulating miR-200c expression. Jin *et al.* (34) have reported that MALAT1 promotes epithelial OC cell proliferation and metastasis *via* modulation of the PI3K-AKT pathway. Wu *et al.* (35) have also shown that MALAT1 is elevated in OC and is involved in cell proliferation, apoptosis, and migration. However, the molecular mechanisms underlying MALAT1 in OC progression, especially the interaction between MALAT1 and miRNA, are not fully understood.

As a member of the polycomb repressive complex 2 complex, PHF19 mediates transcriptional repression of developmental regulatory genes and modulates embryonic stem cell differentiation (36). In mice with rheumatoid arthritis, Phf19 could exert a critical regulatory function to raise germinal center reactions by regulating key molecules associated with proliferation, survival, and differentiation of B cells and follicular helper T cells (37). The expression of PHF19 is also frequently increased in several types of cancer, including colon, skin, lung, rectal, cervical, uterus, and liver cancers (38). Ghislin *et al.* (39) have shown that silence of PHF19 suppresses melanoma cell proliferation and increases the transendothelial migration. In hepatocellular carcinoma, PHF19 promotes tumor growth and is targeted by the tumor-suppressor miR-195-5p (40). In addition, Li *et al.* (41) showed that PHF19 is up-regulated in patient samples with glioblastoma and positively correlated with astrocytoma grades. These findings suggest that PHF19 may be a critical cancer-promoting gene in tumors. However, to the best of our knowledge, the role of PHF19 in OC has not been reported.

In the present study, the expression, function, and interaction of miR-211, MALAT1, and PHF19 in OC were investigated. Our data indicate that miR-211 could inhibit cell proliferation and migration and promote apoptosis by targeting PHF19. Meanwhile, lncRNA MALAT1 antagonized the effect of miR-211 on OC. These results may provide a novel and functional therapeutic target for OC.

MATERIALS AND METHODS

Gene expression and overall survival analyses

We searched the Gene Expression Omnibus (GEO) database (*http://www.ncbi.nlm.nih.gov/geo/*) to obtain microarray profiles. The following strategy was used to search in GEO datasets: (cancer or carcinoma or tumor or neoplasm) and (ovarian). The search results were then specified by using the following filters: GSE [entry type], Homo sapiens [organism]. The resulting records include miRNA microarray and RNA-seq datasets. The datasets were then selected according to the inclusion criteria as follows: miR-211, PHF19, or MALAT1 expression was examined in OC tissues and noncancerous tissues. Data were considered ineligible according to the following exclusion criteria: *1*) miR-211, PHF19, or MALAT1 is not included; *2*) control groups are not included; *3*) cell line samples are used; and *4*) the internal control U6 or glyceraldehyde-3-phosphate dehydrogenase (GAPDH) is not included. The miRNA array expression profile databases GSE83693, GSE61485, GSE47841, GSE53829, GSE52460, and GSE71477 were then obtained to determine the differential expressions of miR-211 between normal ovarian tissues and OC samples. The mRNA array expression profile databases GSE54388, GSE6008, GSE74448, GSE66957, and GSE29450 were selected for exploring the differential expressions of MALAT1 and PHF19. All the primary expression data of miR-211, MALAT1, and PHF19 were normalized by the housekeeping genes U6 (for miR-211) or GAPDH (for MALAT1 and PHF19). All GEO data were further processed by using SPSS 21.0 software (IBM SPSS Statistics, IBM Corp., Armonk, NY, USA), and the unpaired, 2-tailed Student's *t* test was used for statistical analysis.

The overall survival analyses of MALAT1 and PHF19 in OC were assessed according to the mRNA expression profiles with clinical information for patients with OC in The Cancer Genome Atlas (TCGA) data portal (*https://cancergenome.nih.gov/*) and the GEO datasets (*http://www.ncbi.nlm.nih.gov/geo/*). Originally, a total of 1777 OC samples were obtained from the TCGA datasets. Samples were collected according to the following inclusion criteria: *1*) histopathologic diagnosis was OC; *2*) data of samples were available on expression of MALAT1 and PHF19; and *3*) characteristics of patients are available. Data were considered ineligible according to the following exclusion criteria: *1*) first histopathologic diagnosis was not OC; and *2*) patients were diagnosed with other types of cancer except OC. Among these 1777 OC samples, 614 patients with related clinical information were chosen for further analysis. Both the mRNA expression data and clinical characteristics are open-access, and Ethics Committee approval was not needed. To avoid the impact of unrelated causes of death, cases with <1 mo overall survival and death from other diseases or accidents were excluded in this study. Patients were stratified into values below and above the median value (PHF19: low, 309; high, 305; MALAT1: low, 307; high, 307). The data were analyzed by using Kaplan-Meier survival curves and log-rank statistics. We also performed survival analyses for PHF19 and MALAT1 based on individual GEO datasets with PHF19 and MALAT1 expression and clinical information. The inclusion criteria and exclusion criteria were chosen following the TCGA analysis. Three GEO datasets were then selected: GSE9891, GSE26193, and GSE63885.

Quantitative RT-PCR and semiquantitative RT-PCR

Quantitative RT-PCR and semiquantitative RT-PCR were performed as previously described (42). The primers were used as follows: 5′-GTCGTATCCAGTGCAGGGTCCGAGGTATTCGCACTGGATACGACAGGCGA-3′ (miR-211, RT), 5′-GTGCAGGGTCCGAGGT-3′ (miR-universal forward), 5′-GCAAGGGAAACAGTAGGAAG-3′ (miR-211, reverse); 5′-CTCGCTTCGGCAGCACA-3′ (U6, forward), 5′-AACGCTTCACGAATTTGCGT-3′ (U6, reverse); 5′-CTACCTCGGGAAGATCAAGAG-3′ (PHF19, forward), 5′-CTAGGCAGATGTTGCACTTGG-3′ (PHF19, reverse); 5′-GGGTGTTTACGTAGACCAGAACC-3′, (MALAT1, forward), 5′-CTTCCAAAAGCCTTCTGCCTTAG-3′ (MALAT1, reverse); and 5′-GCACCGTCAAGGCTGAGAAC-3′ (GAPDH, forward), 5′-ATGGTGGTGAAGACGCCAGT-3′ (GAPDH, reverse).

miRNA mimic and siRNA transfection

Transfection with miRNA mimic or siRNA was performed by using Lipofectamine RNAiMAX (Thermo Fisher Scientific, Waltham, MA, USA) according to the manufacturer's manual. The siRNA sequences of MALAT1 were as follows: si-MALAT1-1: 5′-TCTAGATTTTTCTTAACAG-3′ (sense), 5′-CTGTTAAGAAAAATCTAGA-3′ (antisense); si-MALAT1-2: 5′-GATCCATAATCGGTTTC-3′ (sense), 5′-GAAACCGATTATGGATC-3′ (antisense); and si-PHF19: 5′-CACCTCAAGTCATCTATCA-3′ (sense), 5′-TGATAGATGACTTGAGGTG-3′ (antisense).

Lentiviral shRNAs and PHF19 overexpressed lentivirus

pGCSIL-PUR lentivirus encoding human MALAT1 short hairpin RNA (shRNA) (sh-MALAT1) and PHF19 shRNA (sh-PHF19) and Lenti-OE lentivirus overexpressing PHF19 were constructed by GeneChem (Shanghai, China) and applied for indicated experiments following the manufacturer's protocols. The oligonucleotides synthesized for construction of these shRNAs were as follows: sh-MALAT1: 5′-CCGGCCGATCCATAATCGGTTTCCTCGAGGAAACCGATTATGGATCGGTTTTTG-3′ (sense), 5′-AATTCAAAAACCGATCCATAATCGGTTTCACTCGAGGAAACCGATTATGGATCGG-3′ (anti-sense); and sh-PHF19: 5′-CCGGCCCACCTCAAGTCATCTATCACTCGAGTGATAGATGACTTGAGGTGGGTTTTTG-3′ (sense), 5′-AATTCAAAAACCCACCTCAAGTCATCTATCACTCGAGTGATAGATGACTTGAGGTGGG-3′ (anti-sense).

Cell proliferation assay

An MTT assay was applied for determining the cell proliferation rate. Briefly, HEY-T30 and SKOV3 cells (5×10^3) were seeded in a 96-well plate and cultured for indicated times. After that, 40 μl of MTT reagent (100 mg/ml; Beyotime, Shanghai, China) were added into the treated cells with 200 μl of culture medium. After 4 h of incubation at 37°C, the supernatant was removed. Then, 150 μl of DMSO (MilliporeSigma, Shanghai, China) were added into the plates for 15 min to dissolve the product of formazan. The optical density was evaluated by using a microplate reader (Molecular Devices, Sunnyvale, CA, USA) at 570 nm following the manufacturer's instruction.

Cellomics staining

The cellomics method was performed to evaluate the proliferation rate of SKOV3 cells infected with PHF19 shRNA. Briefly, 20,000 SKOV3 cells infected with PHF19 shRNA (labeled with green fluorescent protein) or control shRNA were seeded into 96-well plates and incubated at 37°C with 5% CO_2. Plates were processed with the ArrayScan high-content screening software (Thermo Fisher Scientific) for each day's analysis.

Colony formation assay

Treated cells (500 cells/well) were seeded into the 6-well plate in triplicate with complete culture medium. Twelve days later, the colonies were fixed with 4% paraformaldehyde (MilliporeSigma) and stained by 0.04% crystal violet (MilliporeSigma). Individual colonies with >50 cells were counted.

Determination of apoptosis

The percentages of apoptotic cells were evaluated by using the Annexin V-FITC apoptosis detection kit (Beyotime) according to manufacturer's protocol. Briefly, treated cells were harvested and washed twice with 1 time PBS. The cells were then resuspended in 100 μl of 1 time staining buffer with 5 μl Annexin V and incubated for 30 min. Stained cells were examined within 1 h by using the BD FACSCalibur flow cytometer (BD Biosciences, San Jose, CA, USA) and analyzed by using FlowJo 7.6.5 software (Tree Star, Inc., Ashland, OR, USA).

Boyden chamber transwell migration assay

Treated cells (5×10^4 cells/well) were harvested and resuspended into the upper chamber of an insert containing 200 μl of culture medium with 1% FBS. Culture medium with 10% FBS were added into the lower chamber of each insert. After 24 h incubation, the nonmigrating cells were removed with cotton wool. The migrated cells in the lower surface were fixed by using 4% paraformaldehyde (MilliporeSigma) for 30 min and stained with 0.1% crystal violet (MilliporeSigma) for 15 min. Stained cells were photographed under the microscope (Carl Zeiss, Thornwood, NY, USA). The stained crystal violet was then dissolved with 33% acetic acid (MilliporeSigma) and measured by using a microplate reader (Molecular Devices) at 570 nm.

Western blot

Western blot was performed as described previously (42). The following primary antibodies were used: PHF19 (77271, 1:1000; Cell Signaling Technology, Beverly, MA, USA), E-Cadherin (ab219332, 1:2000; Abcam, Cambridge, MA, USA), Vimentin (ab92547, 1:2000; Abcam), and β-ACTIN (TA-09, 1:3000; Zhongshan Golden Bridge Biotechnology, Beijing, China).

Luciferase reporter assay

The cDNA fragment of MALAT1 and the 3′-UTR segment of PHF19 were cloned into the downstream of *Renilla* luciferase reporter of psiCheck2 vector (Promega, Madison, WI, USA) at the *SgfI* and *PmeI* restriction enzyme recognition sites. Luciferase reporter assays were determined by using the psiCheck2 dual luciferase system (Promega) following the manufacturer's instructions. The Fast Mutagenesis System (Beyotime) was applied for construction of MALAT1 and PHF19 3′-UTR reporter gene plasmids with a mutant (mut) miR-211 binding site. Primers were as follows: 5′-GCGCGATCGCCAACCACACGGAGGAGGCGAG-3′ (MALAT1-wild type (WT), forward),

5′-GCGTTTAAACGAAATTGTCTCAATTTGGCTATC-3′ (MALAT1-WT, reverse); 5′-TCGTACTGAGGTGTGGGA-AAGTTTATATGGGGACGTAGGCC-3′ (MALAT1-mut, forward), 5′-GGCCTACGTCCCCATATAAACTTTCCCACACCTCAGT-ACGA-3′ (MALAT1-mut, reverse); 5′-GCGCGATCGCCACTT-CCAGGGCCCAGGTGC-3′ (PHF19-WT, forward), 5′-GC-GTTTAAACGAGGCCACAGCAGCAGTTG-3′ (PHF19-WT, reverse); and 5′-ATCATTTGGTTCCCTCGGGAAAGGGCC-CTTGCCAGTGGGGGTTTG-3′ (PHF19-mut, forward), 5′-CAAACCCCCACTGGCAAGGGCCCTTTCCCGAGGGAA-CCAAATGAT-3′ (PHF19-mut, reverse).

Subcutaneous xenograft growth experiment

In vivo xenograft experiments were performed following the guidelines of the Animal Care and Use Committee of Zhejiang Chinese Medical University. SKOV3 cells (1×10^7) transfected control in shRNA, MALAT1 shRNA, PHF19 shRNA, control miRNA antagomir, or miR-211 antagomir were subcutaneously injected into the right side of the flank area of 6-wk-old female BALB/c nude mice for 44 d. Tumor volumes were evaluated ($0.5 \times \text{length} \times \text{width}^2$) in indicated days after palpable tumors appeared.

Prediction of miRNA binding sites

The online software TargetScan v.7.1 (*http://www.targetscan.org/vert_71/*) was applied for searching the potential binding sites of miR-211.

Statistical analysis

Statistical analysis was conducted by using GraphPad Prism 5 (GraphPad Software, San Diego, CA, USA) and IBM SPSS 22.0. Differences between the 2 groups were statistically analyzed by using the unpaired, 2-tailed Student's *t* test, and values of $P < 0.05$ were considered statistically different. ANOVA was used in cases in which >2 groups were being compared. Correlation between expression levels of MALAT1 and PHF19 was determined by using Spearman's correlation test. To evaluate the prognostic value of PHF19 and MALAT1 expression in patients with OC from the TCGA dataset, the log-rank test and univariate Cox regression analysis were performed.

RESULTS

miR-211 suppresses cellular proliferation, migration, and xenograft growth and induces apoptosis in OC

Initially, to explore the role of miR-211 in the formation and progression of OC, we evaluated the expression of miR-211 in OC tissues compared with normal ovarian tissues. The results showed that miR-211 expression was significantly lower in OC tissues compared with those in normal ovarian specimens (Supplemental Fig. S1*A* and S2*A–F*). We next overexpressed miR-211 in HEY-T30 and SKOV3 cells by transfecting miR-211 mimic (**Fig. 1*A, B***). Colony formation and MTT assay were performed to determine the effect of miR-211 on the proliferation of HEY-T30 and SKOV3 cells. Compared with the control group, the colony number and the MTT absorbance of cells transfected with miR-211 mimic were dramatically decreased (Fig. 1*C–G*). These results suggest that miR-211 inhibits the proliferation of HEY-T30 and SKOV3 cells. To evaluate the role of miR-211 in programmed cell death in OC, the incidence of apoptosis after overexpression of miR-211 was confirmed by using flow cytometry. The results showed that ectopic expression of miR-211 markedly increased cellular apoptosis (Fig. 1*H, I*). In addition, migration assay indicated that transfection with miR-211 mimic significantly inhibited migration both in HEY-T30 and SKOV3 cells (Fig. 1*J, K*). To further investigate the tumor-suppressing effect of miR-211 *in vivo*, a subcutaneous SKOV3 xenograft tumor model was established to investigate the influence of miR-211 on the tumor growth ability. This model showed that the growth rate and average volumes of SKOV3 xenograft tumors were markedly reduced by overexpression of miR-211 using agomir (Fig. 1*L–N*).

PHF19 is a direct target of miR-211 in OC

To explore the potential target genes of miR-211, bioinformatics analysis was performed by using TargetScan v.7.1. The results predicted that miR-211 may target the 3′-UTR region of PHF19 (**Fig. 2*A***). To determine whether the 3′-UTR of PHF19 is a direct target of miR-211 in OC, we then constructed a luciferase reporter vector containing the 3′-UTR region of PHF19 or a mut sequence and cotransfected them into HEY-T30 and SKOV3 cells along with control mimic or miR-211 mimic. Overexpression of miR-211 significantly decreased the luciferase activity of Rellina reporter genes with the WT 3′-UTR region of PHF19 (Fig. 2*B, C*). These changes were diminished in cells transfected with mut 3′-UTR vector. Furthermore, quantitative RT-PCR and Western blot were performed to evaluate the effect of miR-211 on PHF19 expression. The results indicate that overexpression of miR-211 (Fig. 2*D*) markedly suppressed the expression of PHF19 both in mRNA (Fig. 2*E, F*) and in protein (Fig. 2*G, H*) levels.

Silence of PHF19 suppresses cellular proliferation, migration, and xenograft growth and promotes programmed cell death in HEY-T30 and SKOV3 cells

Based on the GEO database analysis, we found that the relative expression of PHF19 was significantly upregulated in OC tissues compared with control healthy specimens (Supplemental Fig. S1*B* and S2*G–K*). To elucidate the precise role of PHF19 in OC, we then evaluated whether PHF19 expression correlates with prognosis in OC in the TCGA cohort and 3 individual GEO datasets. In 614 patients in the TCGA cohort, higher levels of PHF19 expression were significantly correlated with shorter survival times (**Fig. 3*A***). Similar observations were seen in the GEO datasets: GSE9891, GSE26193, and GSE63885 (Supplemental Fig. S3*A–C*). We then transfected PHF19 siRNA into SKOV3 cells

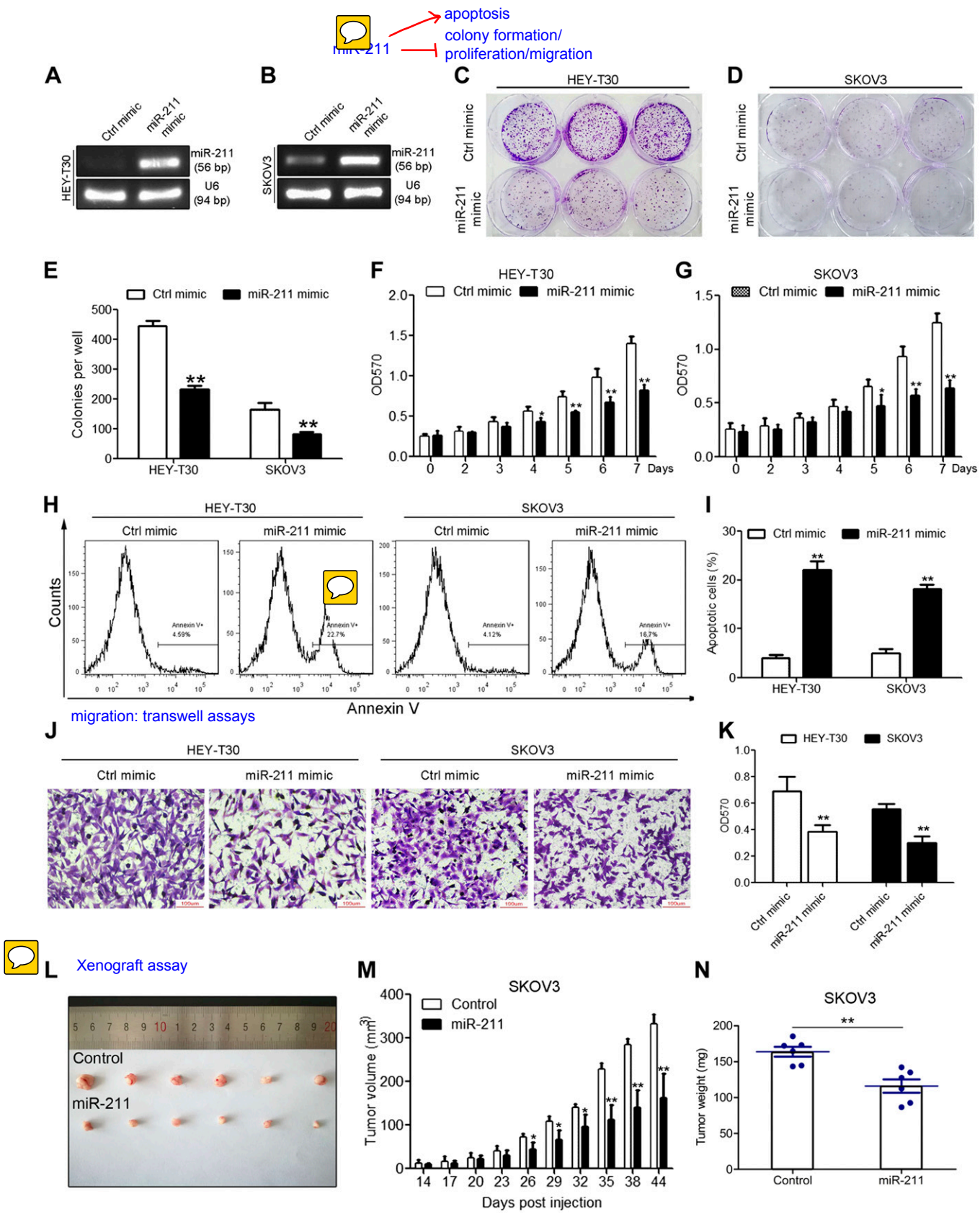

Figure 1. Overexpression of miR-211 suppresses cell proliferation, migration, and xenograft growth and induces cell apoptosis in OC. *A*, *B*) Semiquantitative RT-PCR to determine the expression of miR-211 after transient transfection with miRNA-211 mimic (100 nM) in HEY-T30 (*A*) and SKOV3 (*B*) cells, respectively. *C*, *D*) MiR-211 overexpression decreases the colony formation rate of HEY-T30 (*C*) and SKOV3 (*D*) cells. Representative photographs of the colony formation assay are shown. *E*) The relative colony formation numbers are shown. Data are means ± SD. Three independent experiments were performed, and each experiment contains 3 replicates. An unpaired, 2-tailed Student's *t* test was conducted to analyze the differences between the control and miR-211 groups, $^{**}P < 0.01$ *vs.* control mimic. *F*, *G*) MTT assay to demonstrate the proliferation rate of 100 nM of miR-211

(*continued on next page*)

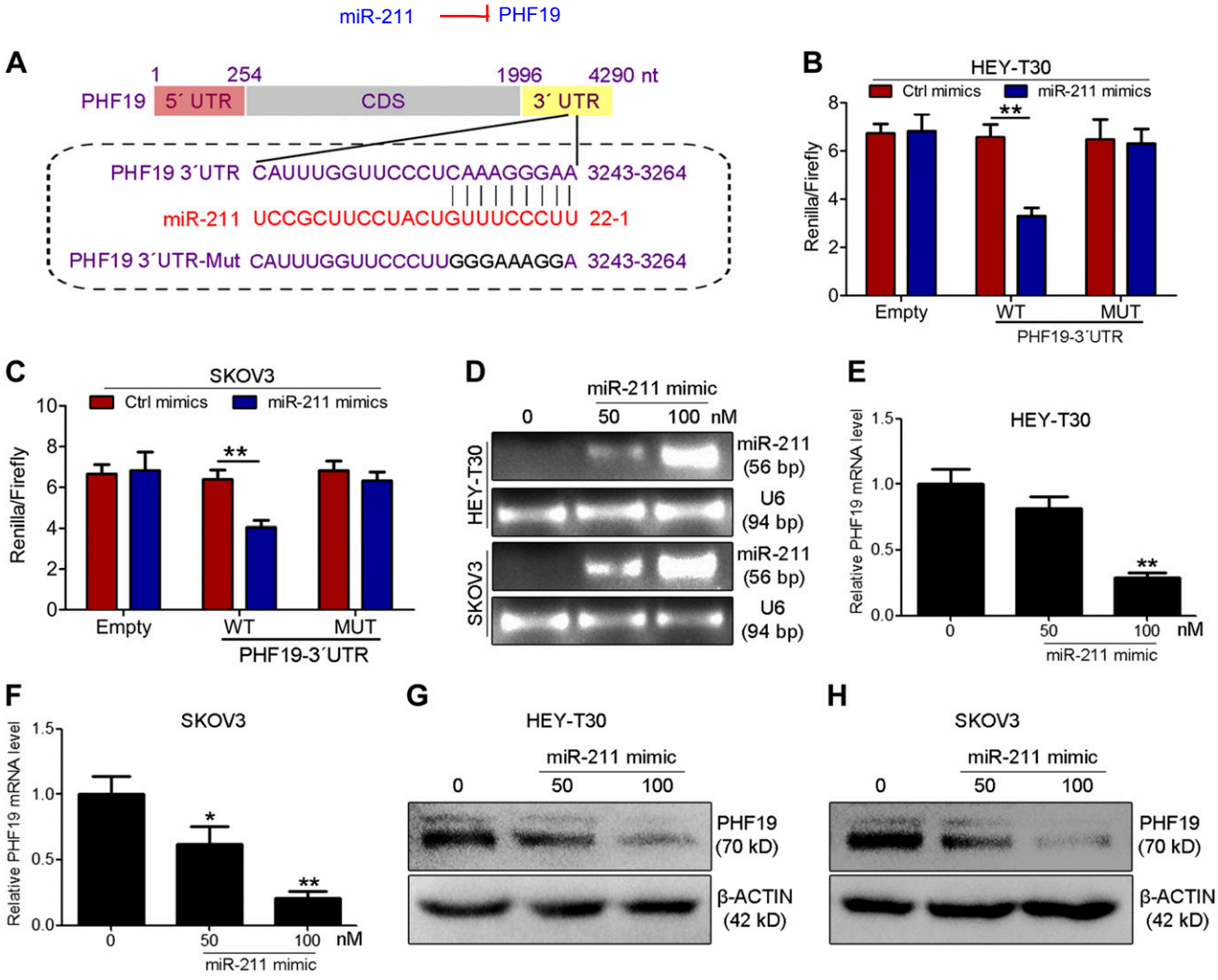

Figure 2. MiR-211 directly targets the 3′-UTR of PHF19. *A*) Schematic view to show the potential binding sites (3243–3264) for miR-211 in the 3′-UTR of the human PHF19 gene (PHF19 3′-UTR-WT). The mutated sequence is shown below (PHF19 3′-UTR-mut). *B, C*) Effect of miR-211 overexpression with 100 nM of miR-211 mimic on the luciferase reporter activity of psiCHECK2-PHF19 3′-UTR-WT and psiCHECK2-PHF19 3′-UTR-mut. HEY-T30 (*B*) and SKOV3 (*C*) cells cotransfected with either miR-211 mimic (100 nM) or control mimic along with psiCHECK2-PHF19 3′-UTR-WT and psiCHECK2-PHF19 3′-UTR-mut. The *Renilla* luciferase activities were assessed at 48 h after transfection, and the firefly luciferase activities were used as internal control. Data are means ± SD, $n = 6$; unpaired, 2-tailed Student's *t* test. $^{**}P < 0.01$ *vs.* control mimic. *D*) Semiquantitative RT-PCR to determine the expression of miR-211 in HEY-T30 and SKOV3 cells with miR-211 mimic (50 or 100 nM) or control mimic transfection. *E, F*) Quantitative RT-PCR analysis of PHF19 mRNA expression in HEY-T30 (*E*) and SKOV3 (*F*) cells transfected with control or miR-211 mimic (50 or 100 nM). Data are means ± SD, 3 independent experiments were performed and each experiment contains 3 replicates; unpaired, 2-tailed Student's *t* test. $^{*}P < 0.05$, $^{**}P < 0.01$, *vs.* control mimic. *G, H*) Western blot detecting PHF19 protein level in control or miR-211 mimic transfected HEY-T30 (*G*) and SKOV3 (*H*) cells.

and evaluated its effect on cell proliferation. Colony formation assay showed that silence of PHF19 reduced the colony numbers compared with the control group in HEY-T30 and SKOV3 cells (Fig. 3*B, C*). Cellomics analysis also showed that a significant decreased number of cells was counted in the group infected with PHF19 lentivirus compared with the control group (Fig. 3*D, E*). Furthermore, silence of PHF19 markedly

mimic-transfected HEY-T30 (*F*) and SKOV3 (*G*) cells. Data are means ± SD, $n = 6$; unpaired, 2-tailed Student's *t* test. $^{*}P < 0.05$, $^{**}P < 0.01$ *vs.* control mimic. *H, I*) Transfection with 100 nM of miR-211 mimic in HEY-T30 and SKOV3 cells induces cellular apoptosis. Quantitative analysis of apoptosis was shown. Data are means ± SD; 3 independent experiments were performed and each experiment contains 3 replicates, unpaired, 2-tailed Student's *t* test. $^{**}P < 0.01$ *vs.* control mimic. *J, K*) Overexpression of miR-211 with miR-211 mimic suppresses cellular migration ability in HEY-T30 and SKOV3 cells, which was determined by using a transwell assay. Scale bars, 100 μm. Data are means ± SD, $n = 6$; unpaired, 2-tailed Student's *t* test. $^{**}P < 0.01$ *vs.* control mimic. *L–N*) SKOV3 cells transfected with miR-211 agomir or control agomir were subcutaneously injected into female BALB/c nude mice. Representative xenografts from each cohort are illustrated (*L*). Transfection with miR-211 agomir significantly inhibited tumor growth (*M*). Weight comparison of xenografts from *L* is shown in *N*. Data = means ± SD, $n = 6$; unpaired, 2-tailed Student's *t* test. $^{*}P < 0.05$, $^{**}P < 0.01$ *vs.* control mimic.

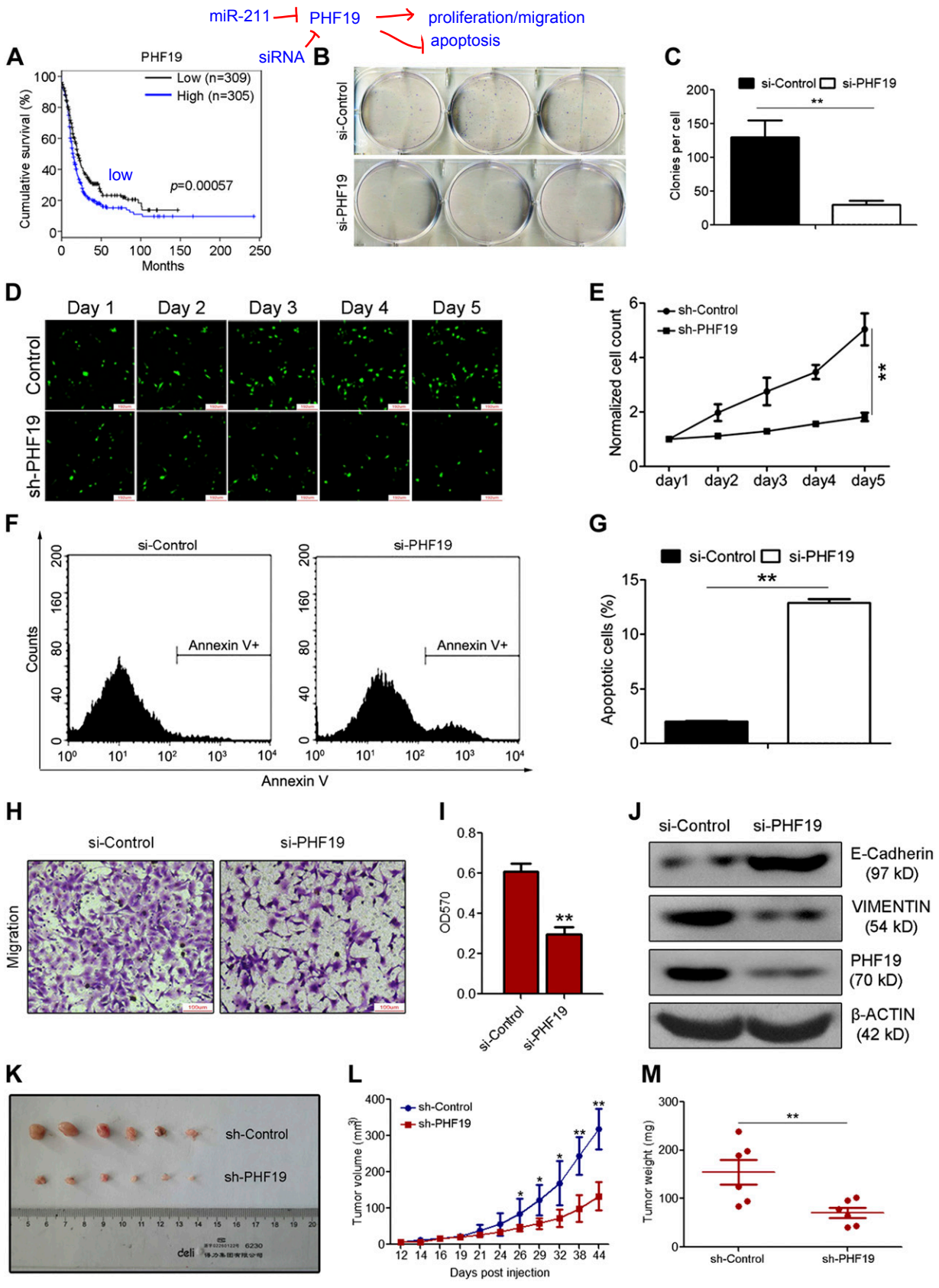

Figure 3. Silence of PHF19 in SKOV3 cells suppresses cell proliferation, migration, and xenograft growth and induces cellular apoptosis. *A*) Kaplan-Meier plot of overall survival in subjects with low (n = 309) *vs.* high (n = 305) PHF19 mRNA expression. Higher levels of PHF19 expression are associated with worse prognosis in OC. Log-rank tests and univariate Cox regression analysis were performed, P = 0.00057. *B*, *C*) Effect of silence of PHF19 (transfected with 100 nM of siRNA) on the colony formation of SKOV3 cells, which were determined by using colony formation assay. Data are means ± SD, 3 independent experiments were performed and each experiment contains 3 replicates; unpaired, 2-tailed Student's t test. $^{**}P < 0.01$ *vs.* control

(*continued on next page*)

induced cell apoptosis in SKOV3 (Fig. 3*F*, *G*). To investigate the role of PHF19 in OC progression, migration assay was performed in SKOV3 cells transfected with PHF19 siRNA. The results indicate that silence of PHF19 significantly suppressed cell migration (Fig. 3*H*, *I*). Western blot analysis revealed that PHF19 knockdown up-regulated the epithelial marker E-cadherin and down-regulated the mesenchymal marker VIMENTIN (Fig. 3*J*). *In vivo* xenograft assay also indicated that silence of PHF19 with PHF19 shRNA lentivirus in SKVO3 cells significantly suppressed tumor growth (Fig. 3*K–M*). Taken together, these studies suggest that PHF19 may act as an oncogene in OC.

PHF19 overexpression counteracted the suppressive role of miR-211 in OC

To investigate whether overexpression of PHF19 can counteract the function of miR-211 in OC, we cotransfected miR-211 mimic (**Fig. 4*A***) and PHF19 overexpressed lentivirus (Fig. 4*B*) into SKOV3 cells. We found that PHF19 overexpression restored cell proliferation suppressed by miR-211 mimic (Fig. 4*C*) and ameliorated apoptosis promoted by miR-211 (Fig. 4*D*, *E*). Meanwhile, ectopic expression of PHF19 promoted cell migration, which was arrested by miR-211 (Fig. 4*F*, *G*). These findings indicate that PHF19 overexpression counteracts the inhibitory function of miR-211 in OC.

miR-211 is sponged by MALAT1 in OC

Accumulating studies have shown that lncRNAs can interact with miRNAs *via* miRNA response elements and regulate each other's expression. We therefore used the bioinformatics database starBase v2.0 (*http://starbase.sysu.edu.cn/*) to search for the potential lncRNA(s) that can sponge miR-211. Interestingly, MALAT1, a well-known oncogenic lncRNA, has a potential binding site for miR-211 (**Fig. 5*A***). Subsequently, we investigated the correlation between miR-211 and MALAT1 in HEY-T30 and SKOV3 cells. To confirm the direct binding potential between MALAT1 and miR-211, a luciferase assay was performed. The MALAT1 fragment containing predicted miR-211 binding site or its mut type was fused into the downstream of the Rellina reporter gene in the psiCHECK2 vector. A significant decrease of luciferase activity was observed when the MALAT1-WT vector was cotransfected with the miR-211 mimic but not with the control miRNA mimic (Fig. 5*B*, *C*). This decrease was diminished in cells cotransfected with miR-211 mimic and MALAT1-mut. In addition, semiquantitative RT-PCR showed that transfection with miR-211 mimic in HEY-T30 and SKOV3 cells significantly suppressed the mRNA level of MALAT1 (Fig. 5*D*, *E*). Moreover, silence of MALAT1 dramatically decreased the expression of PHF19 both in mRNA (Fig. 5*F*, *G*) and protein (Fig. 5*H*, *I*) levels. Taken together, these data indicate that MALAT1 may function as an inducer of PHF19 *via* sponging miR-211.

MALAT1 functions as an oncogenic lncRNA in OC

Based on analysis of the GEO database, we found that MALAT1 expression was up-regulated in OC tissues compared with normal ovarian tissues, although the *P* value was slightly higher than 0.05 ($P = 0.0595$) (Supplemental Fig. S1*C* and Fig. S2*L–P*). We also evaluated whether MALAT1 are related to PHF19 in these clinical samples. A significant positive correlation was noted between MALAT1 and PHF19 (Supplemental Fig. S1*D*). Meanwhile, TCGA cohort analysis showed that higher expression of MALAT1 was correlated with shorter survival times for patients with OC (**Fig. 6*A***). A similar observation was seen in the GEO datasets: GSE9891, GSE26193, and GSE63885 (Supplemental Fig. S3*D–F*). To confirm the role of MALAT1 in OC, we further knocked down the expression of MALAT1 in SKOV3 cells (Fig. 6*B*, *C*). The results show that silence of MALAT1 significantly inhibited cell proliferation (Fig. 6*D*) and colony formation ability in SKOV3 cells (Fig. 6*E*, *F*). Moreover, an increasing number of apoptotic cells were observed in MALAT1-silenced SKOV3 cells (Fig. 6*G*, *H*). In addition, silence of MALAT1 also dramatically suppressed the migration of SKOV3 cells (Fig. 6*I*, *J*). *In vivo*, the xenograft experiment showed that infection with MALAT1 shRNA lentivirus in SKOV3 cells significantly reduced the tumor growth rate (Fig. 6*K–M*). These data suggest that MALAT1 may be an oncogenic lncRNA in OC.

siRNA. *D*, *E*) Cellomics method was applied to determine the effect of PHF19 knockdown on cell proliferation in SKOV3 cells. Scale bars, 192 μm. Data are means ± SD, $n = 6$; unpaired 2-tailed Student's *t* test. $^{**}P < 0.01$ *vs.* control siRNA. *F*, *G*) Flow cytometry analysis of SKOV3 cells transfected with control or PHF19 siRNA to determine the effect of PHF19 knockdown on cell apoptosis. Data are means ± SD, 3 independent experiments were performed and each experiment contains 3 replicates; unpaired, 2-tailed Student's *t* test. $^{**}P < 0.01$ *vs.* control siRNA. *H*, *I*) SKOV3 cells transfected with control or PHF19 siRNA were subjected to migration assay. Scale bars, 100 μm. Data are means ± SD, $n = 6$; unpaired, 2-tailed Student's *t* test. $^{**}P < 0.01$ *vs.* control siRNA. *J*) Western blot analysis to determine the protein levels of E-Cadherin, Vimetin and PHF19 in SKOV3 cells transfected with control or PHF19 siRNA. *K*) Schematic representation of SKOV3 xenograft tumors after 44 d of injection in the sh-PHF19 and negative control groups. *L*) Tumor growth curve of the SKOV3 xenograft in the sh-PHF19 and negative control groups. *M*) Tumor weights between the sh-PHF19 and negative control groups. Data are means ± SD, $n = 6$; unpaired, 2-tailed Student's *t* test. $^{*}P < 0.05$, $^{**}P < 0.01$ *vs.* control siRNA.

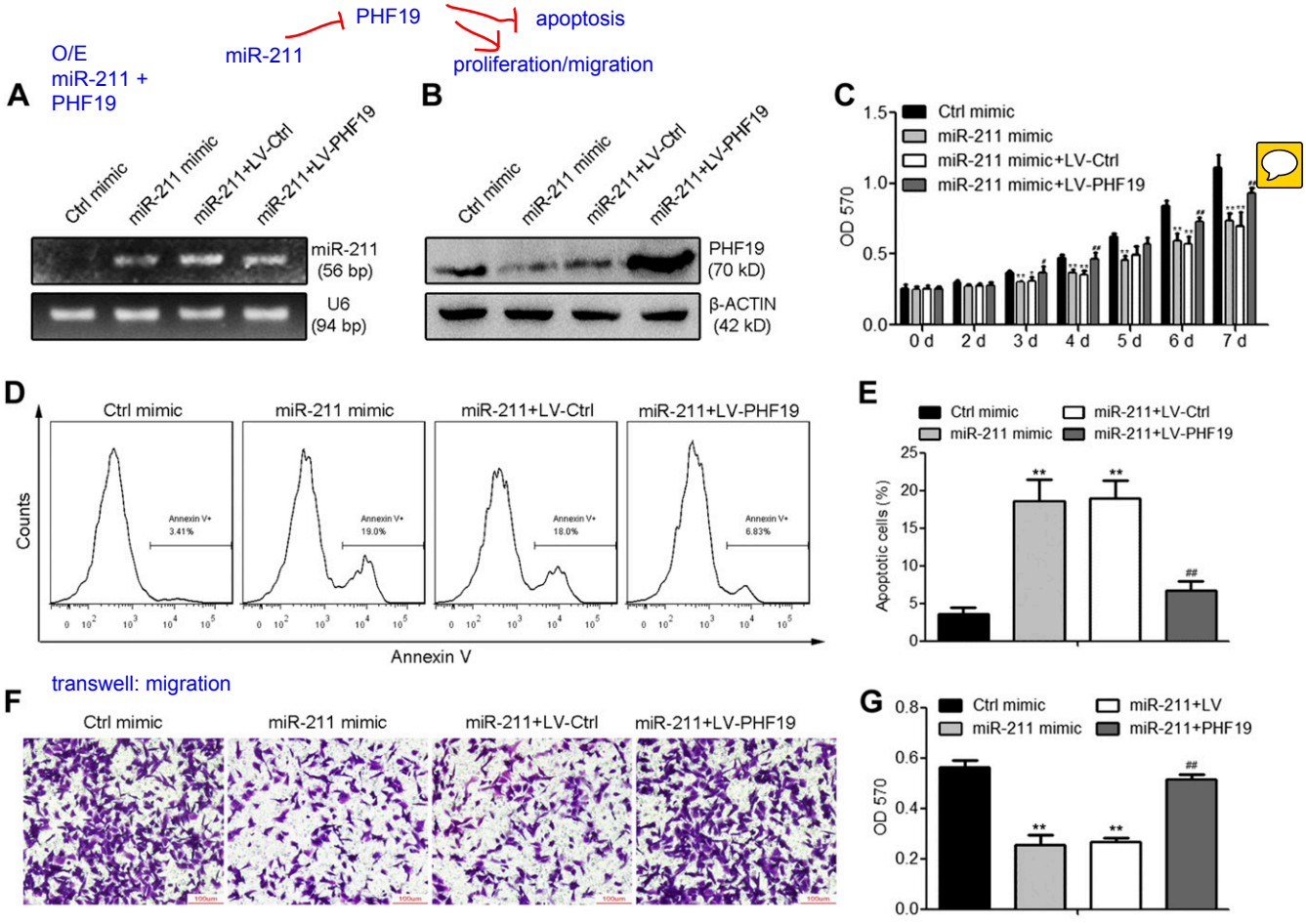

Figure 4. Overexpression of PHF19 antagonizes the suppressive effect of miR-211 on OC. *A*, *B*) The miR-211 and PHF19 expression levels in SKOV3 cells transfected with control mimic or miR-211 mimic (100 nM) with or without infection of PHF19 expression lentivirus, which were determined by using semiquantitative RT-PCR (*A*) and Western blot (*B*). *C*) An MTT assay was performed to determine the cell proliferation abilities of SKOV3 cells with indicated treatment. Data are means ± SD, $n = 6$; statistical analyses were performed by using 1-way ANOVA analysis. $^{*}P < 0.05$; $^{**}P < 0.01$: miR-211 mimic or miR-211+LV-Ctrl *vs.* Ctrl mimic; $^{\#}P < 0.05$; $^{\#\#}P < 0.01$: miR-211+LV-PHF19 *vs.* miR-211+LV-Ctrl. *D*, *E*) FACS analysis revealed apoptotic cells in SKOV3 with indicated treatment (*D*). The percentages of apoptotic cells are summarized in bar charts (*E*). Data are means ± SD. Three independent experiments were performed, and each experiment contains 3 replicates. Statistical analyses were performed by using 1-way ANOVA analysis. $^{**}P < 0.01$: miR-211 mimic or miR-211+LV-Ctrl *vs.* Ctrl mimic; $^{\#\#}P < 0.01$: miR-211+LV-PHF19 *vs.* miR-211+LV-Ctrl. *F*, *G*) Representative images (*F*) and quantification (*G*) of migrated cells in SKOV3 with indicated treatment, which were determined by using transwell migration assay. Data are means ± SD. Three independent experiments were performed, and each experiment contains 3 replicates. Statistical analyses were performed by using 1-way ANOVA analysis. $^{**}P < 0.01$: miR-211 mimic or miR-211+LV-Ctrl *vs.* Ctrl mimic; $^{\#\#}P < 0.01$: miR-211+LV-PHF19 *vs.* miR-211+LV-Ctrl.

Overexpression of PHF19 reverses the suppressive effect of MALAT1 knockdown on SKOV3 cells

We then examined whether ectopic expression of PHF19 attenuates the inhibitory effect of MALAT1 knockdown on OC formation and progression (**Fig. 7*A*, *B***). The MTT assay showed that ectopic expression of PHF19 in SKOV3 cells re-elevated the cell proliferation rate suppressed by MALAT1 siRNA-2 (Fig. 7*C*) and reduced cell apoptosis induced by MALAT1 knock-down (Fig. 7*D*, *E*). In addition, PHF19 overexpression also restored cell migration, which was suppressed by silence of MALAT1 (Fig. 7*F*, *G*). These data indicate that PHF19 may be a critical downstream responsive gene for the function of MALAT1 in OC.

Taken together, these study results reveal that there is a reciprocal repression between MALAT1 and miR-211 in OC (**Fig. 8**). Furthermore, this research highlights the significance of the MALAT1/miR-211/PHF19 axis in tumorigenesis, which adds a new piece of puzzle to the noncoding RNA regulatory networks.

DISCUSSION

In the human genome, ~70% of the DNA sequence is actively transcribed, in which 98% of the transcripts are referred to as noncoding RNAs, and only 2% of RNA sequences encode proteins (43). Noncoding RNAs can be grouped into lncRNAs (>200 nt in length) and small noncoding RNAs (≤200 nt in length), including miRNAs. Mounting evidence has shown that deregulated miRNAs and lncRNAs function as key regulators in the initiation and progression of multiple cancers, including OC, *via* many different pathways (44–46). Our present study, for the first time, revealed a novel ceRNA

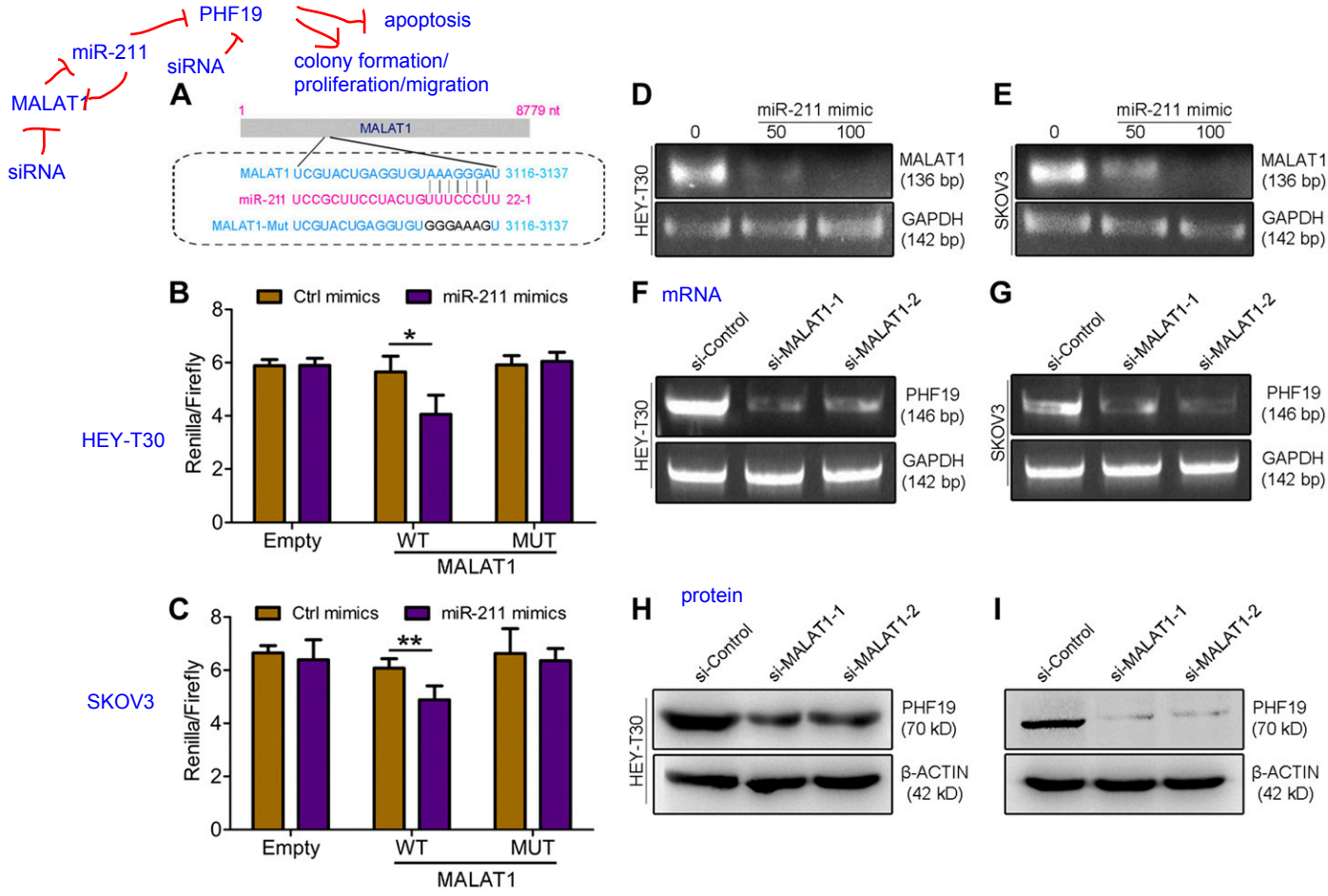

Figure 5. MALAT1 functions as a ceRNA to sponge miR-211. *A*) Schematic view to present the WT and mut binding sites of miR-211 in the mRNA sequence of MALAT1. *B*, *C*) Luciferase assay to determine the direct binding between miR-211 and MALAT1. HEY-T30 and SKOV3 cells were cotransfected with miR-211 mimic (100 nM) or control mimic and luciferase reporter plasmid containing WT binding sites or mut sequence. Data are means ± SD, $n = 6$; unpaired, 2-tailed Student's t test. $^*P < 0.05$, $^{**}P < 0.01$ *vs.* control mimic. *D*, *E*) Semiquantitative RT-PCR to show that overexpression of miR-211 suppresses MALAT1 mRNA level in HEY-T30 (*D*) and SKOV3 (*E*) cells. *F*, *G*) Silence of MALAT1 inhibits the mRNA level of PHF19 in HEY-T30 (*F*) and SKOV3 (*G*) cells, which was evaluated by semiquantitative RT-PCR. *H*, *I*) Western blot analysis indicates that MALAT1 knockdown reduces the protein level of PHF19 in HEY-T30 (*H*) and SKOV3 (*I*) cells.

model, in which the MALAT1/miR-211/PHF19 regulatory axis participate in the pathogenesis of OC. We have found that MALAT1 acts as a ceRNA by sponging miR-211 and potentially rescues the expression of PHF19, thereby promoting the tumorigenesis of OC both *in vitro* and *in vivo*. Elucidation of the MALAT1/miR-211/PHF19 pathway may contribute to the beginnings of a better understanding of OC pathogenesis, and the components of this pathway, MALAT1, miR-211, and PHF19, can be used as novel diagnostic and prognostic markers for clinical prevention and treatment of OC.

miR-211 is abnormally expressed in a wide range of cancers and functions as a tumor-promoting gene or a tumor suppressor (16, 47–50). Searching the literature, Xia *et al.* (16) found that miR-211 arrests cells at the G0/G1 stage, suppresses cellular proliferation, and induces apoptosis. CCND1 and CDK6 are identified as direct targets of miR-211. In this study, by reviewing publicly available microarray results, we found that miR-211 is significantly up-regulated in OC tissues compared with normal controls. In addition, the effect of miR-211 on OC proliferation, apoptosis, and xenograft growth was confirmed, and we further evaluated the role of miR-211 in the migration of OC. Herein, our findings not only revealed the suppressive role of miR-211 OC formation but also demonstrated their inhibitory effect on OC progression.

We next chose to investigate the molecular mechanisms whereby miR-211 suppresses the growth and progression of OC cells, especially its interaction with lncRNAs. LncRNAs are emerging as key players in cancer formation and development. MALAT1, also known as nuclear-enriched transcript 2, is the most well-known lncRNA that plays an important role in the pathogenesis and progression of different tumors (51–56). Elevated expression of MALAT1 promotes cell proliferation, invasion, migration, and metastasis in OC. In the present study, patients with OC and high MALAT1 expression presented with a shorter survival based on TCGA and GEO analyses. In addition, silence of MALAT1 ameliorated the aggressive behavior of OC cells by suppressing cell proliferation and migration and inducing apoptosis. In the next investigation, we evaluated the association of MALAT1 with miR-211 in OC. Importantly, we demonstrated for the first time that MALAT1 suppresses

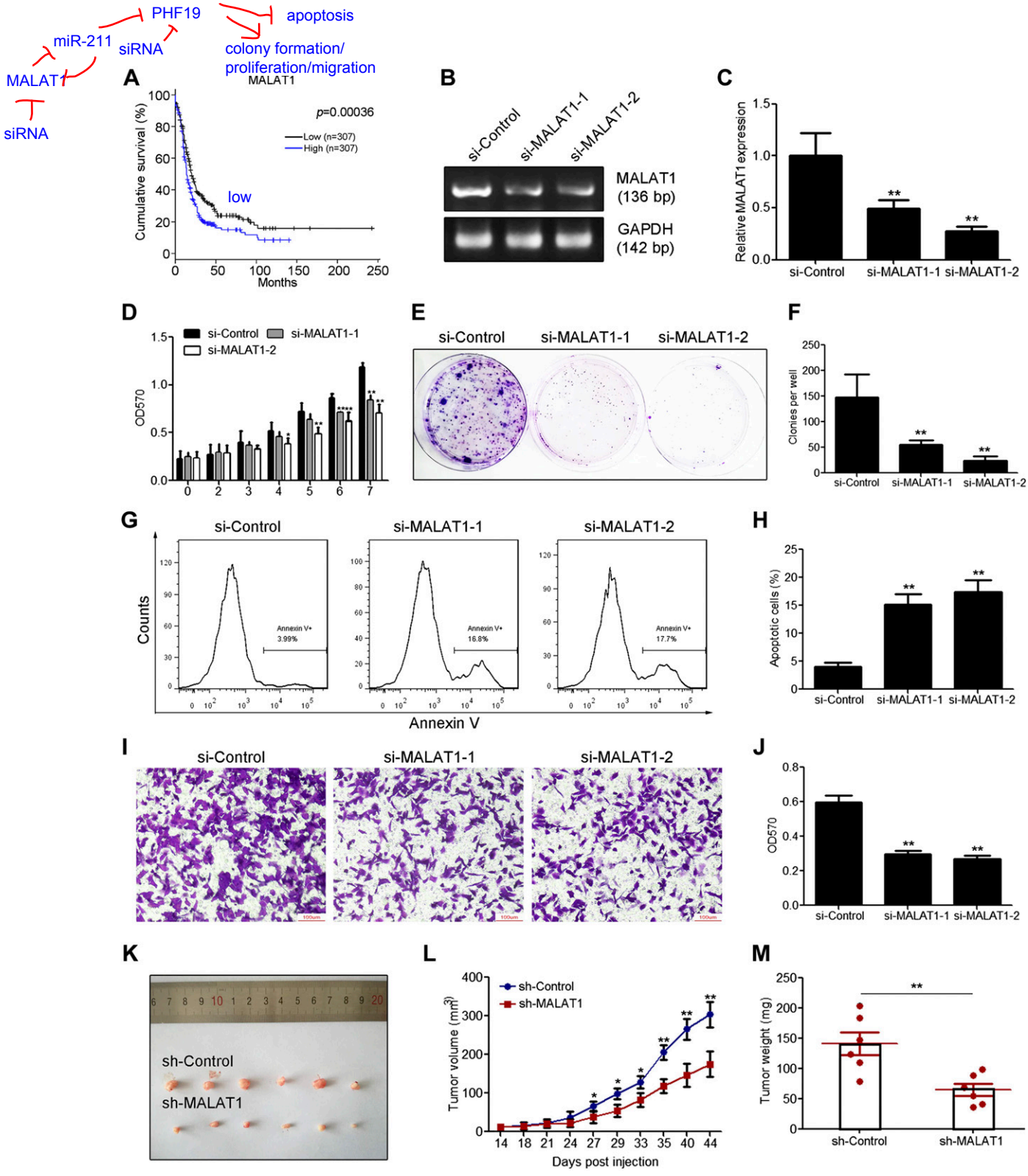

Figure 6. Silence of MALAT1 suppresses SKOV3 cell proliferation, migration, and xenograft growth and induces cell apoptosis. *A*) Correlation between MALAT1 expression and the overall survival of patients with OC, which was shown as Kaplan-Meier survival curves; log-rank tests and univariate Cox regression analysis were performed, $P = 0.00036$. *B, C*) Semiquantitative (*B*) and quantitative (*C*) RT-PCR to evaluate the expression levels of MALAT1 in SKOV3 cells transfected control siRNA or MALAT1 siRNAs (100 nM). *D–F*) Silence of MALAT1 suppresses cell proliferation in SKOV3 cells, which was determined by an MTT (*D*) and a colony formation (*E, F*) assay. Data are means ± SD, $n = 6$; unpaired, 2-tailed Student's t test. $^*P < 0.05$, $^{**}P < 0.01$ *vs.* control siRNA. *G, H*) Flow cytometry analysis indicates that silence of MALAT1 induces apoptosis of SKOV3 cells. Data are means ± SD, 3 independent experiments were performed and each experiment contains 3 replicates; unpaired, 2-tailed Student's t test. $^{**}P < 0.01$ *vs.* control siRNA. *I, J*) Silence of MALAT1 with siRNAs inhibits migration of SKOV3 cells. Data are means ± SD, $n = 6$; unpaired, 2-tailed Student's t test. $^{**}P < 0.01$ *vs.* control siRNA. *K*) Depletion of MALAT1 with shRNA lentivirus shows inhibitory effect in the OC mouse model. *L, M*) Effect of MALAT1 knockdown on the growth (*L*) and weight (*M*) of xenografts derived from SKOV3 cells. Data are means ± SD, $n = 6$; unpaired 2-tailed Student's t test. $^*P < 0.05$, $^{**}P < 0.01$.

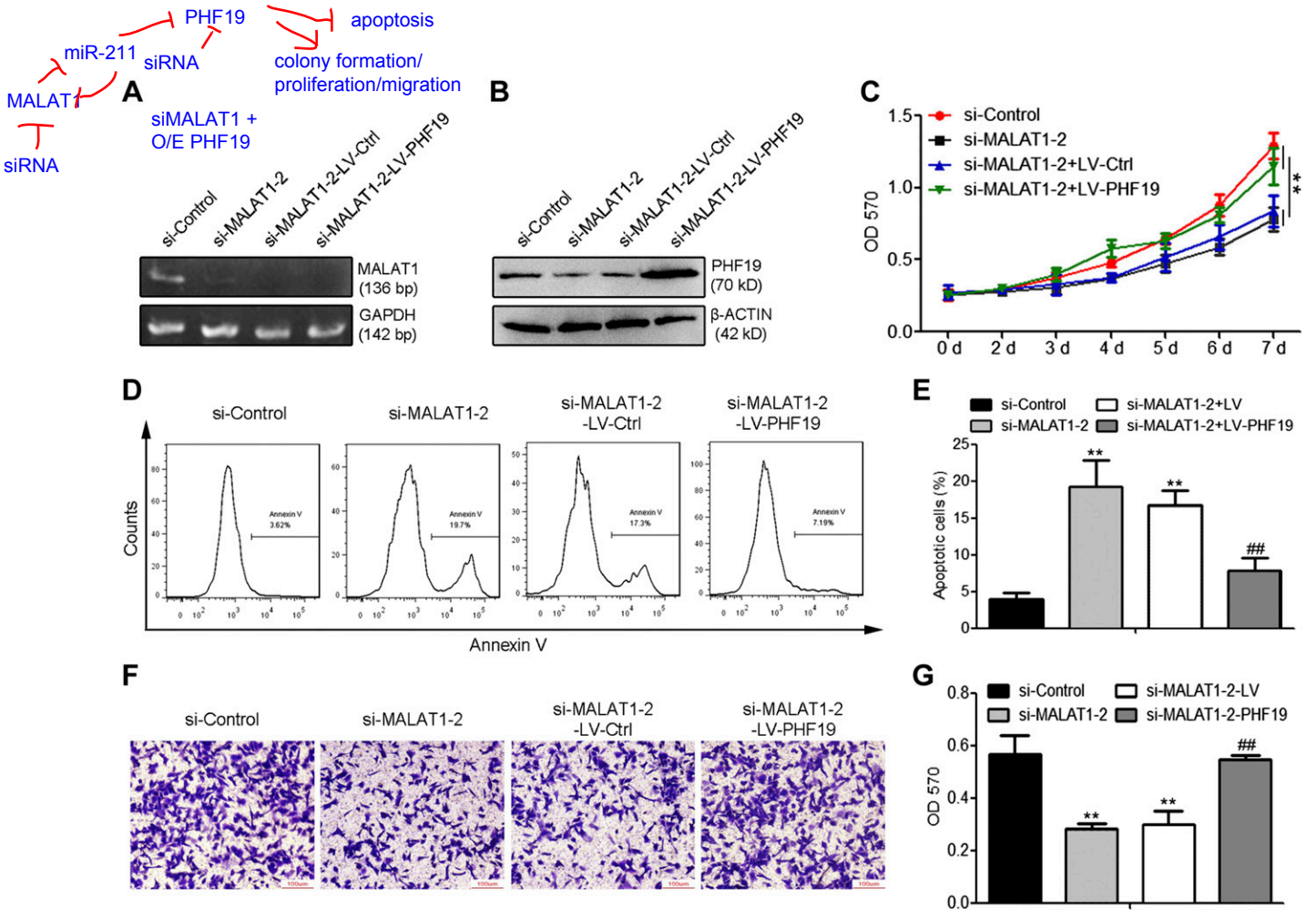

Figure 7. Overexpression of PHF19 attenuates the suppressive function of MALAT1 knockdown in the progression of OC. *A*) Semquantitative RT-PCR to determine the expression of MALAT1 in SKOV3 cells transfected with control siRNA or MALAT1 siRNA2 (100 nM) with or without PHF19 overexpression lentivirus. *B*) SKOV3 cells were transfected with control siRNA or MALAT1 siRNA2 with or without PHF19 expression lentivirus and subjected to Western blot analysis to determine the expression of PHF19. *C*) An MTT assay to evaluate the proliferation rate of SKOV3 cells with indicated treatment. Data are means ± SD, $n = 6$; statistical analyses were performed by using 1-way ANOVA analysis. $^{**}P < 0.01$: si-MALAT1-2 or si-MALAT1-2+LV-Ctrl *vs.* si-Control or si-MALAT1-2+LV-PHF19. *D*, *E*) Percentages of apoptotic cells were analyzed with flow cytometry in SKOV3 cells with indicated treatment. *F*, *G*) Transwell assay to determine the migration ability of SKOV3 cells with indicated treatment. Scale bar, 100 μm. Data are means ± SD. Three independent experiments were performed, and each experiment contains 3 replicates. Statistical analyses were performed by using 1-way ANOVA analysis. $^{**}P < 0.01$: si-MALAT1-2 or si-MALAT1-2+LV-Ctrl *vs.* si-Control; $^{\#\#}P < 0.01$: si-MALAT1-2+LV-PHF19 *vs.* si-MALAT1-2+LV-Ctrl.

miR-211 by acting as a sponge in OC and MALAT1/miR-211 interaction plays an important role in the progression of OC.

As a component of polycomb repressive complex 2, PHF19 is a pivotal member of the polycomb group of proteins to maintain the repressive transcriptional state of developmental associated genes. PHF19 has been reported to be up-regulated in several cancer types, including colon, skin, lung, rectal, cervical, uterus, and liver cancers (38). For instance, Xu *et al.* (40) have reported that PHF19 promotes the progression of hepatocellular carcinoma and is regulated by the tumor suppressor miRNA, miR-195-5p. Ghislin *et al.* (39) have indicated that PHF19 and its upstream regulator AKT control the switch of melanoma cells from proliferative to invasive states. With analysis of data downloaded from GEO datasets, the present study indicated that PHF19 expression exhibited significant differences between patients with OC and normal subjects. We also found that PHF19 functions as a direct target of miR-211 and a key regulator to promote OC proliferation, migration, and xenograft growth, which suggest that PHF19 may be a critical oncogene in OC. However, diagnosis and targeted therapy based on the PHF19 require further molecular research.

There are several limitations to the present study. First, a positive correlation between PHF19 and MALAT1 was shown in this study by using the Pearson test of selected GEO datasets. Meanwhile, for the effect of MALAT1 on PHF19, silence of MALAT1 was found to suppress PHF19 expression in HEY-T30 and SKOV3 cells both in mRNA and protein level (Fig. 5*F–I*). However, because the total length of MALAT1 is 8779 nt, and it is difficult to overexpress MALAT1 ectopically, the effect of MALAT1 overexpression on PHF19 in OC cells was not evaluated in the present study. Second, we only verified the MALAT1/miR-211/PHF19 axis in OC cell lines,

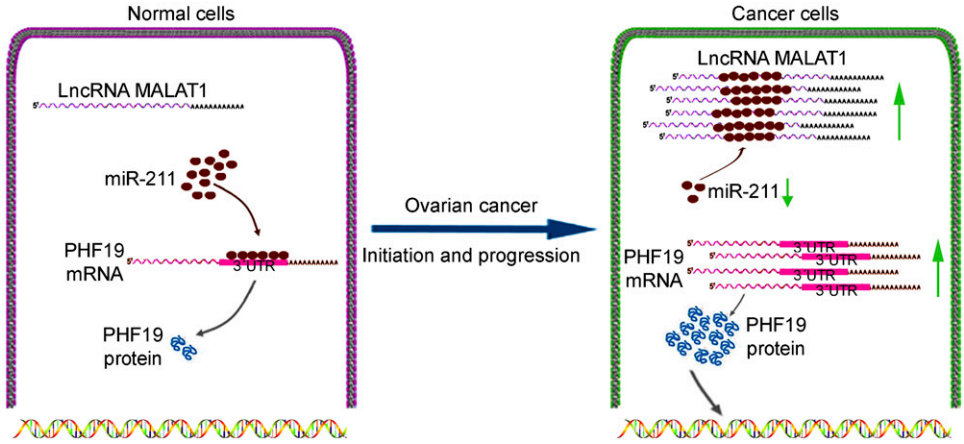

Figure 8. A schematic diagram illustrating the involvement of MALAT1/miR-211/PHF19 axis in OC formation and progression. In OC, lncRNA MALAT1 is highly expressed and sequesters miR-211, thus releasing suppression on the PHF19 mRNA. Elevated expression of PHF19 expression leads to increased production of PHF19 proteins, which promotes the occurrence and progression of OC.

which might not fully reflect the precise processes *in vivo* and which should be confirmed in animal models. Third, apart from OC carcinogenesis, the present findings regarding the MALAT1/miR-211/PHF19 axis must still be verified in other cancer types and biologic processes. In addition, as a member of polycomb group proteins, PHF19 functions to maintain the repressive state of developmental genes and cell cycle regulators (36, 57). The effect of MALAT1 and miR-211 on PHF19 downstream genes needs to be further investigated in future studies.

In summary, our findings indicate that MALAT1 may improve PHF19 expression by competing for miR-211, subsequently mediating OC formation and progression. FJ

ACKNOWLEDGMENTS

This work was supported by the National Natural Science Foundation of China (81302896), the Zhejiang Provincial Public Welfare Project (2016C37056), and the China Postdoctoral Science Foundation (2018M630694). F.T. and X.T. share first authorship. The authors declare no conflicts of interest.

AUTHOR CONTRIBUTIONS

Z. Zhang designed the study; F. Tao, X. Tian, S. Ruan, and Z. Zhang performed the experiments; F. Tao, M. Shen, and Z. Zhang analyzed the data; and X. Tian and Z. Zhang wrote the manuscript.

REFERENCES

1. Hennessy, B. T., Coleman, R. L., and Markman, M. (2009) Ovarian cancer. *Lancet* **374**, 1371–1382
2. Testa, U., Petrucci, E., Pasquini, L., Castelli, G., and Pelosi, E. (2018) Ovarian cancers: genetic abnormalities, tumor heterogeneity and progression, clonal evolution and cancer stem cells. *Medicines (Basel)* **5**
3. Worku, T., Bhattarai, D., Ayers, D., Wang, K., Wang, C., Rehman, Z. U., Talpur, H. S., and Yang, L. (2017) Long non-coding RNAs: the new horizon of gene regulation in ovarian cancer. *Cell. Physiol. Biochem.* **44**, 948–966
4. Deb, B., Uddin, A., and Chakraborty, S. (2018) miRNAs and ovarian cancer: an overview. *J. Cell. Physiol.* **233**, 3846–3854
5. Lou, W., Liu, J., Gao, Y., Zhong, G., Chen, D., Shen, J., Bao, C., Xu, L., Pan, J., Cheng, J., Ding, B., and Fan, W. (2017) MicroRNAs in cancer metastasis and angiogenesis. *Oncotarget* **8**, 115787–115802
6. Mahdian-Shakib, A., Dorostkar, R., Tat, M., Hashemzadeh, M. S., and Saidi, N. (2016) Differential role of microRNAs in prognosis, diagnosis, and therapy of ovarian cancer. *Biomed. Pharmacother.* **84**, 592–600
7. Pal, M. K., Jaiswar, S. P., Dwivedi, V. N., Tripathi, A. K., Dwivedi, A., and Sankhwar, P. (2015) MicroRNA: a new and promising potential biomarker for diagnosis and prognosis of ovarian cancer. *Cancer Biol. Med.* **12**, 328–341
8. Zaman, M. S., Maher, D. M., Khan, S., Jaggi, M., and Chauhan, S. C. (2012) Current status and implications of microRNAs in ovarian cancer diagnosis and therapy. *J. Ovarian Res.* **5**, 44
9. Lv, T., Song, K., Zhang, L., Li, W., Chen, Y., Diao, Y., Yao, Q., and Liu, P. (2018) MiRNA-34a decreases ovarian cancer cell proliferation and chemoresistance by targeting HDAC1. [E-pub ahead of print] *Biochem. Cell Biol.* doi: 10.1139/bcb-2018-0031
10. Cheng, Y., Ban, R., Liu, W., Wang, H., Li, S., Yue, Z., Zhu, G., Zhuan, Y., and Wang, C. (2018) MiRNA-409-3p enhances cisplatin-sensitivity of ovarian cancer cells by blocking the autophagy mediated by Fip200 [E-pub ahead of print]. *Oncol. Res.*
11. Vitiello, M., Tuccoli, A., D'Aurizio, R., Sarti, S., Giannecchini, L., Lubrano, S., Marranci, A., Evangelista, M., Peppicelli, S., Ippolito, C., Barravecchia, I., Guzzolino, E., Montagnani, V., Gowen, M., Mercoledi, E., Mercatanti, A., Comelli, L., Gurrieri, S., Wu, L. W., Ope, O., Flaherty, K., Boland, G. M., Hammond, M. R., Kwong, L., Chiariello, M., Stecca, B., Zhang, G., Salvetti, A., Angeloni, D., Pitto, L., Calorini, L., Chiorino, G., Pellegrini, M., Herlyn, M., Osman, I., and Poliseno, L. (2017) Context-dependent miR-204 and miR-211 affect the biological properties of amelanotic and melanotic melanoma cells. *Oncotarget* **8**, 25395–25417
12. Yu, H., and Yang, W. (2016) MiR-211 is epigenetically regulated by DNMT1 mediated methylation and inhibits EMT of melanoma cells by targeting RAB22A. *Biochem. Biophys. Res. Commun.* **476**, 400–405
13. De Luca, T., Pelosi, A., Trisciuoglio, D., D'Aguanno, S., Desideri, M., Farini, V., Di Martile, M., Bellei, B., Tupone, M. G., Candiloro, A., Regazzo, G., Rizzo, M. G., and Del Bufalo, D. (2016) miR-211 and MITF modulation by Bcl-2 protein in melanoma cells. *Mol. Carcinog.* **55**, 2304–2312
14. Boyle, G. M., Woods, S. L., Bonazzi, V. F., Stark, M. S., Hacker, E., Aoude, L. G., Dutton-Regester, K., Cook, A. L., Sturm, R. A., and Hayward, N. K. (2011) Melanoma cell invasiveness is regulated by miR-211 suppression of the BRN2 transcription factor. *Pigment Cell Melanoma Res.* **24**, 525–537
15. Levy, C., Khaled, M., Iliopoulos, D., Janas, M. M., Schubert, S., Pinner, S., Chen, P. H., Li, S., Fletcher, A. L., Yokoyama, S., Scott, K. L., Garraway, L. A., Song, J. S., Granter, S. R., Turley, S. J., Fisher, D. E., and Novina, C. D. (2010) Intronic miR-211 assumes the tumor suppressive function of its host gene in melanoma. *Mol. Cell* **40**, 841–849
16. Xia, B., Yang, S., Liu, T., and Lou, G. (2015) miR-211 suppresses epithelial ovarian cancer proliferation and cell-cycle progression by targeting Cyclin D1 and CDK6. *Mol. Cancer* **14**, 57
17. Lin, C., and Yang, L. (2018) Long noncoding RNA in cancer: wiring signaling circuitry. *Trends Cell Biol.* **28**, 287–301

18. Slaby, O., Laga, R., and Sedlacek, O. (2017) Therapeutic targeting of non-coding RNAs in cancer. *Biochem. J.* **474**, 4219–4251
19. Pa, M., Naizaer, G., Seyiti, A., and Kuerbang, G. (2017) Long noncoding RNA MALAT1 functions as a sponge of MiR-200c in ovarian cancer [E-pub ahead of print]. *Oncol. Res.*
20. Kuang, D., Zhang, X., Hua, S., Dong, W., and Li, Z. (2016) Long non-coding RNA TUG1 regulates ovarian cancer proliferation and metastasis via affecting epithelial-mesenchymal transition. *Exp. Mol. Pathol.* **101**, 267–273
21. Wu, D. I., Wang, T., Ren, C., Liu, L., Kong, D., Jin, X., Li, X., and Zhang, G. (2016) Downregulation of BC200 in ovarian cancer contributes to cancer cell proliferation and chemoresistance to carboplatin. *Oncol. Lett.* **11**, 1189–1194
22. Li, J., Yang, C., Li, Y., Chen, A., Li, L., and You, Z. (2017) LncRNA GAS5 suppresses ovarian cancer by inducing inflammasome formation [E-pub ahead of print]. *Biosci. Rep.*
23. Li, J., Huang, H., Li, Y., Li, L., Hou, W., and You, Z. (2016) Decreased expression of long non-coding RNA GAS5 promotes cell proliferation, migration and invasion, and indicates a poor prognosis in ovarian cancer. *Oncol. Rep.* **36**, 3241–3250
24. Song, C., Zhang, J., Qi, H., Feng, C., Chen, Y., Cao, Y., Ba, L., Ai, B., Wang, Q., Huang, W., Li, C., and Sun, H. (2017) The global view of mRNA-related ceRNA cross-talks across cardiovascular diseases. *Sci. Rep.* **7**, 10185
25. Li, M. J., Zhang, J., Liang, Q., Xuan, C., Wu, J., Jiang, P., Li, W., Zhu, Y., Wang, P., Fernandez, D., Shen, Y., Chen, Y., Kocher, J. A., Yu, Y., Sham, P. C., Wang, J., Liu, J. S., and Liu, X. S. (2017) Exploring genetic associations with ceRNA regulation in the human genome. *Nucleic Acids Res.* **45**, 5653–5665
26. Qi, X., Zhang, D. H., Wu, N., Xiao, J. H., Wang, X., and Ma, W. (2015) ceRNA in cancer: possible functions and clinical implications. *J. Med. Genet.* **52**, 710–718
27. Tay, Y., Karreth, F. A., and Pandolfi, P. P. (2014) Aberrant ceRNA activity drives lung cancer. *Cell Res.* **24**, 259–260
28. Karreth, F. A., and Pandolfi, P. P. (2013) ceRNA cross-talk in cancer: when ce-bling rivalries go awry. *Cancer Discov.* **3**, 1113–1121
29. An, J., Lv, W., and Zhang, Y. (2017) LncRNA NEAT1 contributes to paclitaxel resistance of ovarian cancer cells by regulating ZEB1 expression via miR-194. *OncoTargets Ther.* **10**, 5377–5390
30. Liu, J., Peng, W. X., Mo, Y. Y., and Luo, D. (2017) MALAT1-mediated tumorigenesis. *Front. Biosci.* **22**, 66–80
31. Gao, K. T., and Lian, D. (2016) Long non-coding RNA MALAT1 is an independent prognostic factor of osteosarcoma. *Eur. Rev. Med. Pharmacol. Sci.* **20**, 3561–3565
32. Xia, H., Chen, Q., Chen, Y., Ge, X., Leng, W., Tang, Q., Ren, M., Chen, L., Yuan, D., Zhang, Y., Liu, M., Gong, Q., and Bi, F. (2016) The lncRNA MALAT1 is a novel biomarker for gastric cancer metastasis. *Oncotarget* **7**, 56209–56218
33. Miao, Y., Fan, R., Chen, L., and Qian, H. (2016) Clinical significance of long non-coding RNA MALAT1 expression in tissue and serum of breast cancer. *Ann. Clin. Lab. Sci.* **46**, 418–424
34. Jin, Y., Feng, S. J., Qiu, S., Shao, N., and Zheng, J. H. (2017) LncRNA MALAT1 promotes proliferation and metastasis in epithelial ovarian cancer via the PI3K-AKT pathway. *Eur. Rev. Med. Pharmacol. Sci.* **21**, 3176–3184
35. Wu, L., Wang, X., and Guo, Y. (2017) Long non-coding RNA MALAT1 is upregulated and involved in cell proliferation, migration and apoptosis in ovarian cancer. *Exp. Ther. Med.* **13**, 3055–3060
36. Ballaré, C., Lange, M., Lapinaite, A., Martin, G. M., Morey, L., Pascual, G., Liefke, R., Simon, B., Shi, Y., Gozani, O., Carlomagno, T., Benitah, S. A., and Di Croce, L. (2012) Phf19 links methylated Lys36 of histone H3 to regulation of polycomb activity. *Nat. Struct. Mol. Biol.* **19**, 1257–1265
37. Ning, F., Wang, C., Niu, S., Xu, H., Xia, K., and Wang, N. (2018) Transcription factor Phf19 positively regulates germinal center reactions that underlies its role in rheumatoid arthritis. *Am. J. Transl. Res.* **10**, 200–211
38. Wang, S., Robertson, G. P., and Zhu, J. (2004) A novel human homologue of Drosophila polycomblike gene is up-regulated in multiple cancers. *Gene* **343**, 69–78
39. Ghislin, S., Deshayes, F., Middendorp, S., Boggetto, N., and Alcaide-Loridan, C. (2012) PHF19 and Akt control the switch between proliferative and invasive states in melanoma. *Cell Cycle* **11**, 1634–1645
40. Xu, H., Hu, Y. W., Zhao, J. Y., Hu, X. M., Li, S. F., Wang, Y. C., Gao, J. J., Sha, Y. H., Kang, C. M., Lin, L., Huang, C., Zhao, J. J., Zheng, L., and Wang, Q. (2015) MicroRNA-195-5p acts as an anti-oncogene by targeting PHF19 in hepatocellular carcinoma. *Oncol. Rep.* **34**, 175–182
41. Li, G., Warden, C., Zou, Z., Neman, J., Krueger, J. S., Jain, A., Jandial, R., and Chen, M. (2013) Altered expression of polycomb group genes in glioblastoma multiforme. *PLoS One* **8**, e80970
42. Zhang, Z., Zhang, B., Li, W., Fu, L., Fu, L., Zhu, Z., and Dong, J. T. (2011) Epigenetic silencing of miR-203 upregulates SNAI2 and contributes to the invasiveness of malignant breast cancer cells. *Genes Cancer* **2**, 782–791
43. Yamamura, S., Imai-Sumida, M., Tanaka, Y., and Dahiya, R. (2018) Interaction and cross-talk between non-coding RNAs. *Cell. Mol. Life Sci.* **75**, 467–484
44. Hao, N. B., He, Y. F., Li, X. Q., Wang, K., and Wang, R. L. (2017) The role of miRNA and lncRNA in gastric cancer. *Oncotarget* **8**, 81572–81582
45. Guo, L., Peng, Y., Meng, Y., Liu, Y., Yang, S., Jin, H., and Li, Q. (2017) Expression profiles analysis reveals an integrated miRNA-lncRNA signature to predict survival in ovarian cancer patients with wild-type BRCA1/2. *Oncotarget* **8**, 68483–68492
46. Wu, Q., Guo, L., Jiang, F., Li, L., Li, Z., and Chen, F. (2015) Analysis of the miRNA-mRNA-lncRNA networks in ER+ and ER- breast cancer cell lines. *J. Cell. Mol. Med.* **19**, 2874–2887
47. Wang, C. Y., Hua, L., Sun, J., Yao, K. H., Chen, J. T., Zhang, J. J., and Hu, J. H. (2015) MiR-211 inhibits cell proliferation and invasion of gastric cancer by down-regulating SOX4. *Int. J. Clin. Exp. Pathol.* **8**, 14013–14020
48. Ye, L., Wang, H., and Liu, B. (2016) miR-211 promotes non-small cell lung cancer proliferation by targeting SRCIN1. *Tumour Biol.* **37**, 1151–1157
49. Jiang, G., Cui, Y., Yu, X., Wu, Z., Ding, G., and Cao, L. (2015) miR-211 suppresses hepatocellular carcinoma by downregulating SATB2. *Oncotarget* **6**, 9457–9466
50. Chu, T. H., Yang, C. C., Liu, C. J., Lui, M. T., Lin, S. C., and Chang, K. W. (2013) miR-211 promotes the progression of head and neck carcinomas by targeting TGFβRII. *Cancer Lett.* **337**, 115–124
51. Xue, D., Lu, H., Xu, H. Y., Zhou, C. X., and He, X. Z. (2018) Long noncoding RNA MALAT1 enhances the docetaxel resistance of prostate cancer cells via miR-145-5p-mediated regulation of AKAP12 *J. Cell. Mol. Med.* **22**, 3223–3237
52. Toraih, E. A., Ellawindy, A., Fala, S. Y., Al Ageeli, E., Gouda, N. S., Fawzy, M. S., and Hosny, S. (2018) Oncogenic long noncoding RNA MALAT1 and HCV-related hepatocellular carcinoma. *Biomed. Pharmacother.* **102**, 653–669
53. Jiang, L. T., Wan, C. H., Guo, Q. H., Yang, S. J., Wu, J. D., and Cai, J. (2018) Long noncoding RNA metastasis-associated lung adenocarcinoma transcript 1 (MALAT1) promotes renal cell carcinoma progression via sponging miRNA-429. *Med. Sci. Monit.* **24**, 1794–1801
54. Li, S., Ma, F., Jiang, K., Shan, H., Shi, M., and Chen, B. (2018) LncRNA Malat1 Promotes Lung Adenocarcinoma by Directly Interacting with SP1. *Cancer Sci.* **109**, 1346–1356
55. Kwok, Z. H., Roche, V., Chew, X. H., Fadieieva, A., and Tay, Y. (2018) A non-canonical tumor suppressive role for the long non-coding RNA MALAT1 in colon and breast cancers [E-pub ahead of print]. *Int. J. Cancer*
56. Bai, L., Wang, A., Zhang, Y., Xu, X., and Zhang, X. (2018) Knockdown of MALAT1 enhances chemosensitivity of ovarian cancer cells to cisplatin through inhibiting the Notch1 signaling pathway. *Exp. Cell Res.* **366**, 161–171
57. Qin, S., Guo, Y., Xu, C., Bian, C., Fu, M., Gong, S., and Min, J. (2013) Tudor domains of the PRC2 components PHF1 and PHF19 selectively bind to histone H3K36me3. *Biochem. Biophys. Res. Commun.* **430**, 547–553

Received for publication March 14, 2018.
Accepted for publication May 14, 2018.